Earth and Planetary Science Letters, 76 (1985/86) 35–44
Elsevier Science Publishers B.V., Amsterdam – Printed in The Netherlands

[6]

An estimate of hydrothermal fluid residence times and vent chimney growth rates based on ^{210}Pb/Pb ratios and mineralogic studies of sulfides dredged from the Juan de Fuca Ridge

David Kadko [1], Randolph Koski [2], Mitsunobu Tatsumoto [3] and Robin Bouse [2]

[1] *College of Oceanography, Oregon State University, Corvallis, OR 97331 (U.S.A.)*
[2] *U.S. Geological Survey, 345 Middlefield Road, Menlo Park, CA 94025 (U.S.A.)*
[3] *U.S. Geological Survey, Denver, CO 80225 (U.S.A.)*

Received January 22, 1985; revised version received August 26, 1985

The ^{210}Pb/Pb ratios across two sulfide samples dredged from the Juan de Fuca Ridge are used to estimate the growth rate of the sulfide material and the residence time of the hydrothermal fluid within the oceanic crust from the onset of basalt alteration. ^{210}Pb is added to the hydrothermal fluid by two processes: (1) high-temperature alteration of basalt and (2) if the residence time of the fluid is on the order of the 22.3-year half-life of ^{210}Pb, by in-situ growth from ^{222}Rn (Krishnaswami and Turekian, 1982). Stable lead is derived only from the alteration of basalt.

The ^{210}Pb/Pb ratio across one sample was ~ 0.5 dpm/10^{-6} g Pb, and across the other it was ~ 0.4 dpm/10^{-6} g Pb. These values are quite close to the ^{238}U/Pb ratios of basalts from the area, suggesting that the residence time of the hydrothermal fluid from the onset of basalt alteration is appreciably less than the mean life of ^{210}Pb, i.e., the time required for ingrowth from the radon.

An apparent growth rate of 1.2 cm/yr is derived from the slope of the ^{210}Pb/Pb curve for one of the samples. This is consistent with its mineralogy and texture which suggest an accretionary pattern of development. There is no obvious sequential growth pattern, and virtually no gradient in ^{210}Pb/Pb across the second sample. This is consistent with alteration of the original ^{210}Pb/Pb distribution by extensive remobilization reactions which are inferred from the mineralogic and textural relationships of the sample.

1. Introduction

The discovery of large chemical anomalies in the hydrothermal fluids which emanate from vents associated with seafloor spreading centers has had a significant impact on our understanding of the chemical budget of the ocean [1,2]. To comprehend the influence of seawater hydrothermal systems on the composition of ocean water, it is necessary to understand the rate, duration, and possible periodicity of hydrothermal activity at individual vents, as well as the residence time of ocean water within these systems. Similarly, the significance of the very high rate of heat loss via the black smoker vents, as it pertains to the ridge crest heat budget and possibly the lifetime of the axial magma chamber, depends on how long such activity persists at a given locality [3–5].

Sulfide chimney or chimney-type fragments from the East Pacific Rise at 21°N and the Juan de Fuca Ridge are found to contain significant quantities of Cu, Zn, Ag, and Cd [6–9]. From a resource perspective, it is desirable to know how the vent sulfide material forms and how rapidly it accumulates. The preservation of massive sulfide deposits on the seafloor is dependent on the nature of the depositional mechanisms, the rates of accumulation by these mechanisms, and on the rate of chemical weathering prior to burial.

The substantial excess ^{210}Pb ($t_{1/2}$ = 22.3 years) over its parent ^{226}Ra ($t_{1/2}$ = 1622 years) found in hydrothermal vent material is a potential tool for determining the growth rate and lifespan of such deposits. Finkel et al. reported significant excess ^{210}Pb concentrations in sulfide precipitates and vent material from the East Pacific Rise (EPR) at 21°N [10]. These authors compared the ^{210}Pb and ^{210}Po contents of active and inactive vent material and suggested that the cycle of buildup, cessation, and decay by oxidation of these sulfide chimneys

0012-821X/85/$03.30

is measured in tens to a few hundred years. Lalou and Brichet treated the $^{210}Pb/Pb$ ratio of venting particles as an initial ratio and compared this to the $^{210}Pb/Pb$ ratio measured on vent wall material. Assuming instantaneous growth of the chimneys, they found the age of several active vents to be on the order of tens of years [11]. Chung et al. measured the $^{210}Pb/Pb$ ratio across a vent wall and suggested that the growth of such deposits could occur in tens of years or less [12]. These relatively rapid growth rates are consistent with the steep temperature and chemical gradients found at many discharge sites, and with some visual observations [13]. The ages of molluscs collected near hot springs of the Galapagos Rise and the EPR at 21°N have been found to range from 3 to 27 years [14–16]. These ages suggest that some vents may indeed be short-lived on a geologic time scale.

Excess ^{210}Pb in the hydrothermal fluid may also be used to determine the residence time of the hydrothermal fluid within the crust. Krishnaswami and Turekian measured the concentration of ^{210}Pb in vent waters of the Galapagos Rise and suggested that when compared to the rate of ^{210}Pb production from in-situ ^{222}Rn decay and basalt alteration, this information could yield an estimate of the crustal residence time of the hydrothermal fluid from the onset of basalt alteration [17].

In this work, we present ^{210}Pb data for two sulfide and four basalt samples dredged from the Juan de Fuca Ridge. The $^{210}Pb/Pb$ ratios, along with the mineralogic, textural, and chemical characteristics of the sulfides, is used to estimate vent growth rates, fluid residence time, and possible growth histories of these deposits.

2. Sample location

The sulfide samples analyzed in this work were recovered from two locations on the Juan de Fuca Ridge (JDF) (Fig. 1). Sulfide material was dredged from the southern Juan de Fuca Ridge (44°40′N, 130°22′W; water depth 2200 m) in September 1981 by the U.S. Geological Survey vessel "S.P. Lee" [8,9,18], and from the Endeavour segment of the JDF, north of the Cobb Offset (47°57′N, 129°06′W; water depth ~2200 m) in October 1982 by the University of Washington research vessel "T.G. Thompson" [19–22]. Observations conducted from DSRV "Alvin" during the University of Washington's expedition to the Endeavour site in 1984 contributed to the interpretation of our data. The locations of the basalts analyzed in this work are also indicated in Fig. 1.

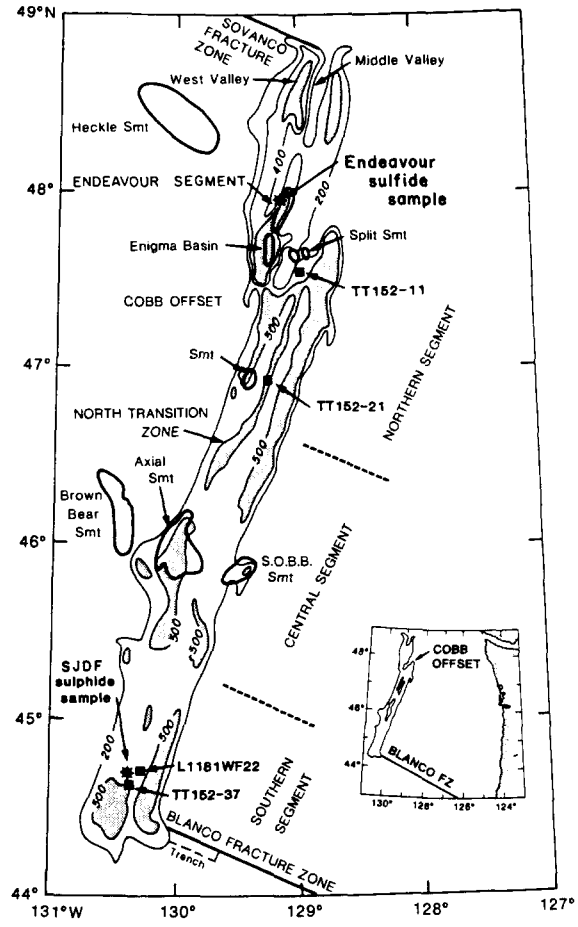

Fig. 1. Location of samples from the Juan de Fuca Ridge analyzed in this study. Sulfide samples are indicated by a star, basalts by a solid square. Contour lines indicate the magnetic anomaly pattern, in gammas [37]. Stippled area is +500 gammas.

3. Methods

Mineral identifications and textural interpretations were made using reflected and transmitted light microscopy, scanning electron microscopy, electron microprobe, and X-ray diffraction techniques. Polished thin sections for petrographic studies were prepared along transects perpendicular to layering in the southern JDF and Endeavour sulfide samples (Fig. 2). Details of the mineralogic

studies are presented elsewhere [9,21,22].

The ^{210}Pb analysis of the sulfides and basalt material was made by counting its daughter product, ^{210}Po ($t_{1/2} = 138.4$ days). Finkel et al. have shown that disequilibrium may exist between ^{210}Pb and ^{210}Po in venting sulfide particles [10]. However, the samples within this study were not fresh particles but were from seafloor constructional sulfide deposits and were analyzed for the polonium 1–2 years after the collection date. During this time, any ^{210}Pb-^{210}Po disequilibrium would be largely eliminated. Approximately 200 mg of each sulfide subsample (obtained along the same transect from which the thin sections were prepared) was dissolved in a mixture of HNO_3, $HClO_4$, and HF to which approximately 25 dpm ^{208}Po standard was added. After the solution was first purged of radon, it was enclosed for a known period of time, and the ingrown radon collected and counted to determine the ^{226}Ra content. The radon is counted within a zinc-sulfide cell housed against a photomultiplier tube. The solution was then taken to dryness, redissolved in 1.5*N* HCl, and the polonium was directly plated onto a silver disk which had been placed onto the bottom of the beaker. The disk was removed, rinsed with distilled water, dried, and placed in an alpha spectrometer system consisting of a silicon surface-barrier detector and a multi-channel analyzer. Details of these procedures can be found elsewhere [23,24]. Lead in the sulfides was determined on duplicate subsamples by atomic absorption spectrometry.

The U, Th and Pb concentrations in basalts were determined by isotope dilution mass spectrometry. About 100 mg of sample was decomposed in a teflon vial using HF-HNO_3 to which a ^{205}Pb-$^{233}U + ^{236}U$-^{230}Th tracer was added. Pb was separated using anion exchange chromatography (100 μl resin volume) in a 1.2 *N* HBr medium. U and Th were separated by an anion exchange resin in a 7*N* HNO_3 medium. Details of this procedure are given by Tatsumoto and Unruh [25]. The ^{230}Th and ^{232}Th were also analyzed by alpha spectrometry. Samples of 1–3 g were dissolved with HF-HNO_3 to which a ^{228}Th tracer was added. The Th was separated in a 7*N* HNO_3 anion exchange column and plated onto stainless steel disks. This method is described in detail by Newman et al. [26]. Though the small sample size (< 3 g) precluded great sensitivity, the ^{232}Th determinations by this method were not greatly different from those values obtained by mass spectrometry (Table 1).

4. Composition, texture, and growth mechanisms

4.1. Southern Juan de Fuca Ridge sample

The massive sulfide sample from the southern Juan de Fuca Ridge (WF-22D-6) is an angular slab approximately 8 cm in thickness, composed largely of granular, dark gray layers rich in Zn sulfide (sphalerite + wurtzite) with thin interlayers and a crust of Fe sulfide (pyrite + marcasite) (Fig. 2a). The Fe-sulfide crust is constructed from overlapping arcuate segments, with the underturned layer extending a short distance into the zone rich in Zn sulfide. The thin (~ 30 μm) veneer of

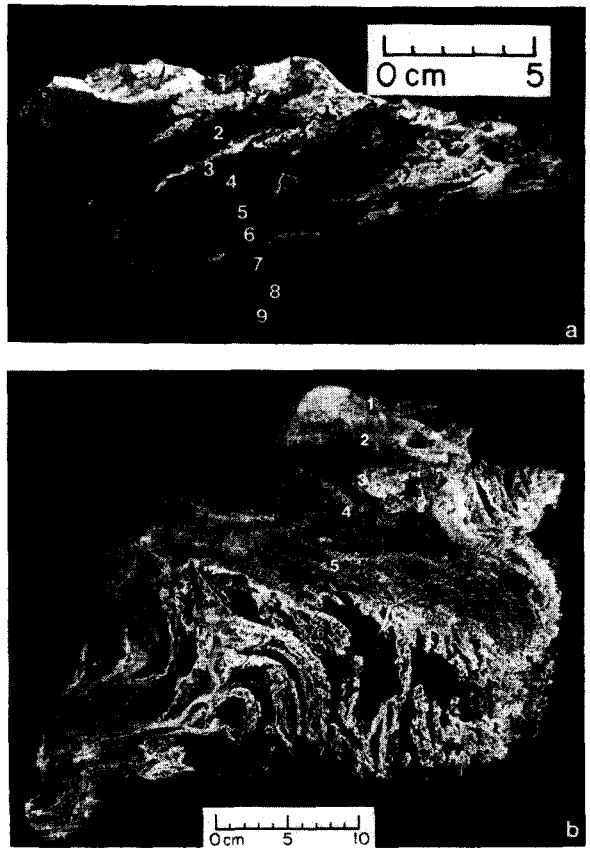

Fig. 2. (a) Cross section of southern Juan de Fuca sample WF-22D-6 showing sampling transect. (b) Cross section of Endeavour sample TT-170-66D-A1 showing sampling transect.

orange-red Fe oxide on the Fe-sulfide crust indicates that this surface was in contact with seawater while on the seafloor. The bottom surface of the Fe-sulfide crust and the Fe-sulfide interlayers have corroded outlines and are partly replaced by Zn sulfide. The interlayers show a progressive decrease in thickness and an increase in corrosion and replacement towards the sample core.

In contrast to the Fe-sulfide outer crust, the opposing Zn-sulfide-rich inner surface is granular and unaltered. The Zn-sulfide phases exhibit a range of textures that result from open-space deposition and replacement of pre-existing sulfide minerals [8]. Textural and mineralogical variations within the Zn-sulfide layers include (1) an increase in the ratio of wurtzite to colloform sphalerite; (2) a decrease in Pb-sulfide minerals; (3) an increase in chalcopyrite; and (4) a coarsening of grain size (of wurtzite and chalcopyrite) toward the core of the sample.

This sample is interpreted to be a fragment from the wall of a sulfide chimney formed at an active or recently active vent site. Koski et al. have proposed that the layering as well as the textural and compositional variations are the result of deposition during episodes of recurrent mixing of discharging hydrothermal fluid and cold ambient seawater [9]. These authors suggest that quench deposition from the initial mixing of seawater and hydrothermal fluid results in a coherent shell of fine-grained, colloform Fe and Zn sulfide enclosing an open network of anhedral sphalerite grains. Thickening of the shell (by outward growth of colloform Fe sulfide and inward growth of colloform Zn sulfide) inhibits the influx of seawater, and the assemblage of euhedral sphalerite, wurtzite, and chalcopyrite is deposited under conditions of increased temperature and decreased pH, f_{S_2}, and f_{O_2}. These higher-temperature minerals replace earlier formed pyrite, sphalerite, and Pb sulfide. The textural progression from colloform and fine-grained sulfide to coarser-grained, euhedral sphalerite and wurtzite indicate a change from rapid crystallization promoted by sudden changes in fluid composition and decreases in temperature to slower crystallization under relatively stable conditions within the sulfide shell.

The multi-layered structure results when high-temperature vent fluid escapes through the sulfide wall, initiating a new cycle of mixing and deposition of a secondary shell rich in Fe sulfide. The corroded appearance of previously deposited sphalerite, galena, and pyrite indicates that these phases undergo re-equilibration with higher temperature fluid; metals (Fe, Pb, and Zn) solubilized at the higher temperatures migrate outward to be redeposited in each newly formed secondary sulfide shell. Fe-sulfide crusts formed earlier are partly consumed, and corroded remnants become incorporated as thin bands during cyclical growth of the sulfide wall.

4.2. Endeavour sulfide sample, northern Juan de Fuca Ridge

The sulfide sample dredged from the Endeavour segment of the Juan de Fuca Ridge (TT-170-66D-A1) lacks open channelways and has greater textural complexity than the southern JDF sample (Fig. 2b). This sample is a representative portion of the very large, massive sulfide structures (up to 20 m high, 30 m long, and 10–15 m across) that were observed during DSRV "Alvin" dives to the area in 1984 and does not include any individual chimney-like spouts [21,22]. Tivey and Delaney suggest that these sulfides have undergone a more complex and evolved history than the southern JDF samples and recognize four distinct textural zones within the sample [21,22]. Zone 1 is a thin (2–3 mm) porous shell composed of fine-grained colloform, dendritic marcasite and interstitial barite and amorphous silica. This outer shell encloses a dense 1-cm-thick area (zone 2) where disequilibrium textural relationships predominate. There is a fine-grained assemblage of intergrown pyrrhotite (partly resorbed and replaced by pyrite), marcasite, wurtzite, and chalcopyrite. Zone 3, approximately 10 cm thick, is characterized by intricate mineralogical layering that exhibits crosscutting relationships and by a complex alternation of bands rich in Zn sulfide and Fe sulfide. Textural zone 4 forms the inner portion of the sample and is a much coarser-grained, porous aggregate of pyrite and marcasite with minor wurtzite and Cu-Fe sulfide.

Tivey and Delaney [22] suggest that the size and complexity of the Endeavour dredge sample can be accounted for by two distinct phases of growth. Phase 1 is analogous to chimney construction at 21°N and the southern JDF in which there is

growth centered around a high-temperature flow. This phase is also observed at the Endeavour site but occurs on top of, or extending out the side of, previously deposited massive sulfide structures. Zone 2 is interpreted to be a remnant of the original quench-textured sulfide wall. The termination of this phase occurs when fluid channels close and flow is redirected. Zone 3 represents fossil hydrothermal flow channels; sealing of exit ports may cause the intricate layering observed in this zone. At this point, vigorous throughflow of hydrothermal fluid is replaced by a diffuse flow through the enclosing walls; such flow was commonly observed emanating from the massive structures during the 1984 "Alvin" program. This flow and associated conductive cooling results in the deposition of amorphous silica in the outer portions of the existing structure (zone 1), which acts to solidify or "cement" the structure, and in the deposition of porous, coarse-grained Fe-sulfide within the inner portion of the sample (zone 4).

Although both the southern JDF and Endeavour samples are fragments of constructional sulfide deposits formed at a hydrothermal vent, their textural characteristics reveal different growth mechanisms. The southern JDF sample is similar to chimney samples from 21°N [27–30] that display an outward zonation from a high-temperature core to a lower-temperature rim assemblage of minerals. It appears to have formed by a series of outward accretions that result in a cyclical growth pattern. Layering in the Endeavour sample is more complex, suggesting a more evolved growth history. There is no concentric growth pattern, and there is a lack of open fluid channels. Although a simple growth pattern may have existed in early stages of sulfide deposition (phase 1), the primary zonation may have been obliterated by the plugging of fluid channels and the redirection of fluids and by mineral deposition "overprinting" during cooling of the hydrothermal fluid by conduction. This later stage of diffuse flow (phase 2) may not only account for the greater textural complexity of the Endeavour sample but also provides a mechanism for the growth of the very large, solid structures that were observed at that site [22].

5. ^{210}Pb in the hydrothermal system

^{210}Pb is added to the hydrothermal fluid by (1) high-temperature alteration of basalt and (2) *if* the residence time of the fluid within the crust from the onset of basalt alteration is on the order of the 22.3-year half-life of ^{210}Pb, by in-situ growth from ^{222}Rn (3.83-day half-life) in the hydrothermal fluid, [17]. Stable lead in the fluid comes only from the alteration of basalt [31]. If it is assumed that the uranium content of basalts is approximately 0.1 dpm/g, that secular equilibrium exists between U and ^{210}Pb, and that the water/rock mass ratio is 3, the concentration of ^{210}Pb in the hydrothermal fluid resulting from basalt alteration alone would be about 33 dpm/kg. Measurements of very high radon concentrations in ridge crest vent waters, on the other hand, indicate that the ^{210}Pb concentration resulting from in-situ growth could be much higher. Dymond et al. [32] extrapolated the low-temperature Galapagos vent radon values to 350°C end-member activities of 10^3–10^4 dpm/kg, though they suggested that these high extrapolated values were an artifact of radon input during low-temperature fluid-crust interaction. From the high-temperature 21°N vents, however, Kim and Finkel extrapolated radon measurements on dilute samples to a 350°C end-member activity of 320 dpm/kg [33], and recently at the DSRV "Alvin" study site on the Endeavour segment of the Juan de Fuca Ridge, radon activities over 800 dpm/kg were measured on vent waters which exceeded 300°C [34]. Using the Endeavour radon value, the ^{210}Pb concentration from in-situ growth from radon would be 800 $(1 - e^{-\lambda\tau})$ dpm/kg, where τ is the residence time of the fluid

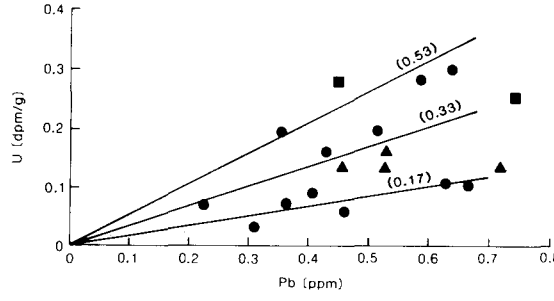

Fig. 3. Uranium and lead concentrations of basalt from the Juan de Fuca Ridge (circles—Church and Tatsumoto [35]; triangles—this study). Parentheses give U/Pb ratio of lines in dpm U/μg Pb.

TABLE 1

Uranium, thorium, and lead analyses on several basalts dredged from the Juan de Fuca Ridge

Sample No.	^{230}Th [a] (dpm/g)	^{210}Pb [a] (dpm/g)	^{232}Th [b] (dpm/g)	^{232}Th [a] (dpm/g)	U [b] (dpm/g)	Pb [b] (ppm)
TT-152-11	0.18 ± 0.03	0.20 ± 0.01	0.123 ± 0.002	0.14 ± 0.02	0.131 ± 0.002	0.461 ± 0.001
47°32.5′N, 128°57.8′W						0.458 ± 0.001
(2640–2690 m)						
TT-152-21	0.23 ± 0.03	0.24 ± 0.02	0.108 ± 0.001	0.15 ± 0.02	0.129 ± 0.002	0.721 ± 0.001
46°55.5′N, 128°15.7′W						0.725 ± 0.001
(2410–2520 m)						
TT-152-37	0.64 ± 0.03	0.41 ± 0.03	0.147 ± 0.002	0.11 ± 0.01	0.161 ± 0.002	0.537 ± 0.001
44°37.1′N, 130°23.4′W						0.520 ± 0.002
(2235–2240 m)						
L1181WF-22-23	0.29 ± 0.04	0.31 ± 0.02	0.112 ± 0.001	0.16 ± 0.03	0.132 ± 0.002	0.532 ± 0.001
44°40.3′N, 130°21.6′W						0.523 ± 0.001
(2208 m)						

[a] Analysis by alpha-spectroscopy; errors are 1σ counting statistics.

[b] Analyses by isotope dilution mass spectrometry. Duplicate analyses were made for Pb. The differences in Pb concentration between duplicate runs are probably due to sample heterogeneity of different chips rather than analytical errors.

and λ is the decay constant of ^{210}Pb (0.031 yr^{-1}). Therefore, if τ is significant with respect to the half-life of ^{210}Pb, in-situ growth from radon in the hydrothermal fluid would be the major source of the ^{210}Pb. Krishnaswami and Turekian [17] noted then that the ^{210}Pb activity of debouching vent water could be used to estimate the residence time of the hydrothermal fluid. They recognized, however, that the extremely low ^{210}Pb activities of their Galapagos samples were probably due to precipitation of Pb within the system. This effect would result in an underestimate of the ^{210}Pb activity and, consequently, the value of τ. For this reason, ^{210}Pb measurements normalized to stable lead would be more useful. Such measurements could be performed on the sulfide deposits which form directly from the venting fluid.

5.1. $^{210}Pb/Pb$ from the basalt source

To estimate the $^{210}Pb/Pb$ ratio to be expected in the sulfide deposit from the basalt alteration process alone (i.e., $\tau = 0$), the U/Pb ratio of basalt samples dredged from the JDF area are plotted in Fig. 3 [35] (Table 1). It is assumed that ^{210}Pb is in secular equilibrium with uranium in the basalt. Values of the $^{230}Th/U$ activity ratio measured on ridge basalts are generally greater than unity but less than 1.5 [26,36] (see also Table 1). High values may be attributed to seawater contamination [26]. For our purposes, this disequilibrium is not significant, and the assumption that $U/^{210}Pb = 1$ does not introduce appreciable error. From Fig. 3, it is seen that the $(U/Pb)_{basalt}$ (hence $(^{210}Pb/Pb)_{basalt}$) ratio is < 0.55 dpm $U/10^{-6}$ g Pb. If the sulfide $^{210}Pb/Pb$ ratio is similar to this, the major source of ^{210}Pb to the system must be the basalt source and not in-situ growth from radon.

5.2. $^{210}Pb/Pb$ from in-situ growth

The growth of the $^{210}Pb/Pb$ ratio from in-situ radon decay, as a function of τ, is shown in Table

TABLE 2

Growth of ^{210}Pb from ^{222}Rn decay in the hydrothermal system

τ [a] (years)	$^{210}Pb_R$ activity [b] (dpm/g)	$^{210}Pb_T/^{210}Pb_B$ [c]
1	0.24 × Pb	1.7
5	1.2 × Pb	4.6
10	2.1 × Pb	7.4
20	3.7 × Pb	12.2

[a] τ = residence time of the hydrothermal fluid from the onset of basalt alteration.

[b] ^{210}Pb in sulfide from radon source, calculated from $8.0(1 - e^{-\lambda\tau}) \times Pb$ where the ^{222}Rn concentration is 800 dpm/kg; λ = decay constant of ^{210}Pb (0.0311 yr^{-1}); Pb = sulfide lead concentration (ppm).

[c] $^{210}Pb_T$ = total ^{210}Pb in sulfide = $^{210}Pb_R + ^{210}Pb_B$; $^{210}Pb_B$ = ^{210}Pb from basalt source only.

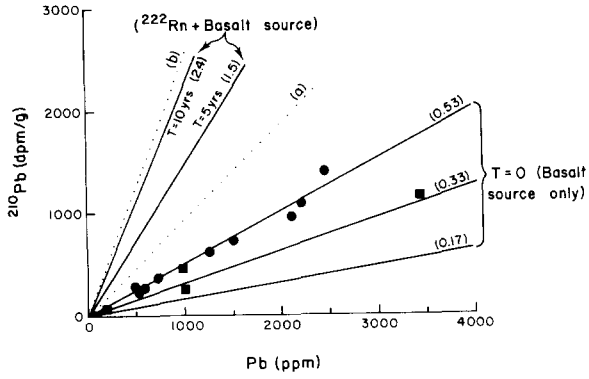

Fig. 4. The ^{210}Pb/Pb ratio expected in a hydrothermal fluid and associated sulfide deposits (assuming U and ^{210}Pb in the basalts to be in secular equilibrium) under several conditions: When T, the residence time of the fluid, equals zero the ^{210}Pb/Pb ratios (in parentheses) are those of the basalts (see Fig. 3). When $T = 5$ and 10 years the ^{210}Pb/Pb ratios reflect in-growth from ^{222}Rn in addition to the basalt source. The solid lines represent the case where the radon concentration is 800 dpm/kg (see Table 2). Dotted line (a) is the case for $T = 5$ years and [Rn] = 400 dpm/kg, (b) for $T = 5$ years and [Rn] = 1600 dpm/kg. Pb and ^{210}Pb determinations from the southern JDF sample (circles) and from the Endeavour Ridge (squares) sulfide samples are shown.

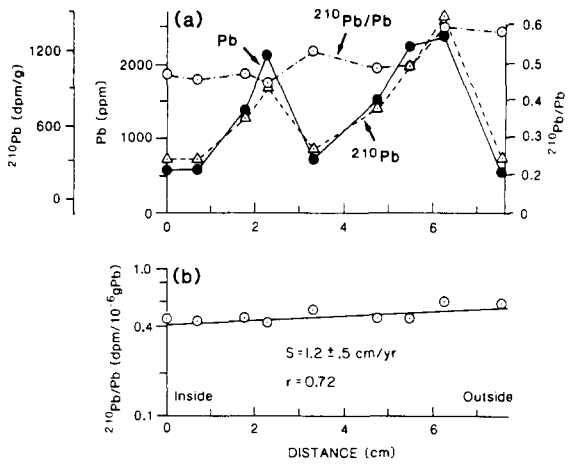

Fig. 5. (a) ^{210}Pb, Pb, and ^{210}Pb/Pb for southern Juan de Fuca sample WF-22D-6 plotted against distance along the transect shown in Fig. 2a. (b) The log of ^{210}Pb/Pb plotted against distance for sample WF-22D-6.

2. The ^{210}Pb/Pb ratio of the fluid from this source would be 8.0 $(1 - e^{-\lambda\tau})$ dpm/ppm if $Pb_{basalt} = 0.3$ ppm, the water/rock ratio is 3, and the Endeavour fluid radon concentration of 800 dpm/kg is used. The ^{210}Pb content of the sulfide from this source alone would then be 8.0 $(1 - e^{-\lambda\tau}) \times Pb_{sulfide}$. The third column in Table 2 shows how the ^{210}Pb from basalt alteration alone, $^{210}Pb = \sim 0.33\ Pb_{sulfide}$ (from Fig. 3), becomes relatively unimportant as the residence time of the fluid increases (see Fig. 4). The effect of higher and lower radon concentration on this calculation are also shown in Fig. 4.

5.3. *^{210}Pb/Pb results from the Juan de Fuca samples*

The ^{210}Pb, ^{226}Ra, Pb, and ^{210}Pb/Pb values for the sulfide samples are presented in Table 3. The ^{226}Ra activities are negligible, and thus the ^{210}Pb activities are the unsupported values. The ^{210}Pb, Pb, and ^{210}Pb/Pb values for the southern JDF sample are plotted in Fig. 5a and for the Endeavour sample in Fig. 6a. In both cases the ^{210}Pb/Pb ratios do not fluctuate markedly across the transect and, as shown in Fig. 4, are within the range expected from ^{210}Pb production from the basalt source alone. This implies a fluid residence time from the onset of basalt alteration which is short compared to the 22.3-year half-life of ^{210}Pb.

In Figs. 5b and 6b, the ^{210}Pb/Pb ratio is plotted on a semi-log scale versus distance along the sam-

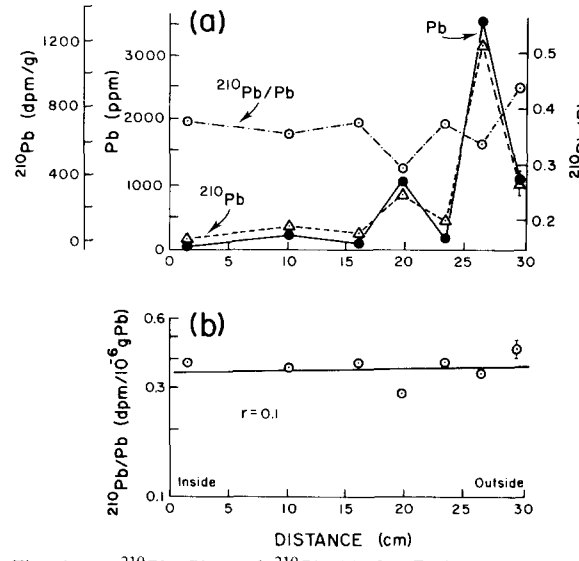

Fig. 6. (a) ^{210}Pb, Pb, and ^{210}Pb/Pb for Endeavour sample TT-170-66D-A1 plotted against distance along the transect shown in Fig. 2b. (b) The log of ^{210}Pb/Pb plotted against distance for sample TT-170-66D-A1.

TABLE 3

^{210}Pb and Pb measurements on Juan de Fuca sulfide samples

Sample No.	^{210}Pb [a] (dpm/g)	Pb [b] (wt.%)	^{210}Pb/Pb (dpm/μg)	^{226}Ra (dpm/g)
Southern Juan de Fuca (WF-22D-6)				
1	292.8 ± 5.6	0.050 ± 0.001	0.59 ± 0.02	n.a.
2	1459.8 ± 20.7	0.244 ± 0.006	0.60 ± 0.02	n.a.
3	1096.8 ± 17.2	0.223 ± 0.006	0.49 ± 0.015	n.a.
4	728.1 ± 11.3	0.149 ± 0.004	0.49 ± 0.015	< 1
5	372.9 ± 6.6	0.072 ± 0.002	0.52 ± 0.02	n.a.
6	954.6 ± 12.4	0.210 ± 0.006 [c]	0.455 ± 0.01	< 1
7	615.6 ± 11.9	0.126 ± 0.003	0.49 ± 0.015	< 1
8	266.6 ± 4.6	0.056 ± 0.001	0.48 ± 0.01	< 1
9	283.4 ± 5.8	0.058 ± 0.002	0.49 ± 0.02	< 1
Endeavour (TT-170-66D-A1) [d]				
1a	499.7 ± 13.1	0.099 ± 0.003	0.44 ± 0.06	n.a.
b	380.9 ± 11.0			
2a	1147.3 ± 48.5	0.348 ± 0.009	0.335 ± 0.02	n.a.
b	1187.3 ± 32.0			
3a	65.9 ± 2.8	0.018 ± 0.001	0.37 ± 0.03	n.a.
b	68.1 ± 3.3			
4	285.4 ± 4.8	0.100 ± 0.003	0.285 ± 0.01	n.a.
5	48.0 ± 1.5	0.013 ± 0.001	0.37 ± 0.03	n.a.
6	67.6 ± 1.9	0.019 ± 0.001	0.36 ± 0.02	n.a.
7	30.0 ± 1.2	0.008 ± 0.001	0.375 ± 0.05	n.a.
Bulk "inside"	56.3 ± 2.1	n.a.	n.a.	1.87 ± 0.38
Bulk "outside"	753.1 ± 10.5	n.a.	n.a.	9.47 ± 0.20

[a] Errors are 1σ counting statistics.
[b] Values are the average of duplicate runs. The errors are the average deviations of the measurements.
[c] No duplicate—assumes a 3% error.
[d] Duplicate ^{210}Pb analyses were performed on samples marked "a" and "b".
n.a. = not analyzed.

pling transect. Assuming, in the case of a short residence time system, that variations of the ^{210}Pb/Pb ratio in the hydrothermal solution is small, then the gradient in ^{210}Pb/Pb for the southern JDF sample (Fig. 5b) could be interpreted as indicating an accretionary growth rate, from the inside out, of 1.2 cm/yr. The concentric progression of alternating zinc-rich and iron-rich layers toward the oxidized iron sulfide crust described earlier is consistent with this interpretation. Replacement textures and the corroded appearance of phases within this sample, however, suggest that some degree of solubilization and remobilization of metals has occurred. Although normalizing the ^{210}Pb to stable Pb will mitigate the effect of such processes, mobilization of metals through layers would tend to "homogenize" the sample. Therefore, this growth rate should be considered an upper limit.

The ^{210}Pb/Pb ratios along the Endeavour sample show virtually no gradient (Fig. 6b). The homogeneity of ^{210}Pb/Pb values across the sample is probably a consequence of extensive remobilization and reprecipitation processes. This resulted from closure and redirection of fluid channelways and corresponding changes in flow rates which led to varying conditions of precipitation. Therefore, the apparent growth rate of over 20 cm/yr which is derived from the slight ^{210}Pb/Pb slope ($r = 0.1$) is most likely an artifact of these processes. This hypothesis is supported by the intricate mineralogical layering of the sample and by the lack of both concentric growth patterns and open fluid channelways.

6. Summary and conclusions

Two sulfide samples dredged from the Juan de Fuca Ridge were analyzed for $^{210}Pb/Pb$ ratios and mineralogic characteristics.

(1) The range of the $^{210}Pb/Pb$ ratios of the sulfide samples (0.285–0.60) are within the range expected if the residence time of the hydrothermal fluid in the crust, from the onset of basalt alteration, is short compared to the 22.3-year half-life of ^{210}Pb.

(2) The sample from the southern JDR displayed a concentric pattern of growth and development, and the $^{210}Pb/Pb$ gradient indicated an apparent growth rate of 1.2 cm/yr. Some degree of remobilization and reprecipitation of constituents may have altered this gradient however; hence this growth rate should be considered an upper limit.

(3) The Endeavour sample displayed no obvious sequential growth pattern, and virtually no gradient in $^{210}Pb/Pb$ across the sample was found. Extensive remobilization reactions probably obliterated the primary zonation as well as the original $^{210}Pb/Pb$ distribution in this sample.

Acknowledgements

We wish to thank J. Dymond, J.R. Delaney, M.K. Tivey, K.L. Von Damm, E. Suess, K. Bencala, and two anonymous reviewers for their helpful criticism and J.R. Delaney and H.P. Johnson for providing the Endeavour sample. This work was supported in part by a National Research Council Fellowship while D.K. was a post-doctoral associate with the U.S. Geological Survey at Menlo Park, and by NSF grant OCE-8315243.

References

1 J.M. Edmond, C. Measures, R.E. McDuff, L.H. Chan, R. Collier, B. Grant, L.I. Gordon and J.B. Corliss, Ridge crest hydrothermal activity and the balances of the major and minor elements in the ocean: The Galapagos data, Earth Planet. Sci. Lett. 46, 1–18, 1979.

2 J.M. Edmond, C. Measures, B. Magnum, B. Grant, F.R. Sclater, R. Collier, A. Hudson, L.I. Gordon and J.B. Corliss, On the formation of metal-rich deposits at ridge crusts, Earth Planet. Sci. Lett. 46, 19–30, 1979.

3 M.J. Mottl, Metabasalts, axial hot springs, and the structures of hydrothermal systems at mid-ocean ridges, Geol. Soc. Am. Bull. 94, 161–180, 1983.

4 K.C. Macdonald, K. Becker, F.N. Spiess and R.D. Ballard, Hydrothermal heat flux of the "black smoker" vents on the East Pacific Rise, Earth Planet. Sci. Lett. 48, 1–7, 1980.

5 D.R. Converse, H.D. Holland and J.M. Edmond, Flow rates in the axial hot springs of the East Pacific Rise (21°N): implications for the heat budget and the formation of massive sulfide deposits, Earth Planet. Sci. Lett. 69, 159–175, 1984.

6 J.L. Bischoff, R.J. Rosenbauer, P.J. Aruscavage, P.A. Baedecker and J.G. Crock, Sea-floor massive sulfide deposits from 21°N, East Pacific Rise, Juan de Fuca Ridge, and Galapagos Rift: bulk chemical composition and economic implications, Econ. Geol. 78, 1711–1720, 1983.

7 C.L. Morgan and B.W. Selk, Ore assays of massive sulfides from three spreading centers, in: Offshore Tech. Conf., 16th Offshore Technical Conference, Paper 477, 12 pp., Houston, Texas, 1984.

8 R.A. Koski, W.R. Normark, J.L. Morton and J.R. Delaney, Metal sulfide deposits on the Juan de Fuca Ridge, Oceanus 25, 42–48, 1982.

9 R.A. Koski, D.A. Clague and E. Oudin, Mineralogy and chemistry of massive sulfide deposits from the Juan de Fuca Ridge, Geol. Soc. Am. Bull. 95, 930–945, 1984.

10 R.C. Finkel, J.D. Macdougall and Y.C. Chung, Sulfide precipitates at 21°N on the East Pacific Rise: ^{226}Ra, ^{210}Pb, and ^{210}Po, Geophys. Res. Lett. 7, 685–688, 1980.

11 C. Lalou and E. Brichet, Ages and implications of East Pacific Rise sulfide deposits at 21°N, Nature 300, 169–171, 1982.

12 Y. Chung, R. Finkel and K. Kim, Hydrothermal ^{210}Pb on the East Pacific Rise at 21°N, EOS, Trans. Am. Geophys. Union 62, 913, 1981.

13 M.S. Goldfarb, D.R. Converse, H.D. Holland and J.M. Edmond, The genesis of hot spring deposits on the East Pacific Rise, 21°N, in: The Kmoko and Related Volcanogenic Massive Sulfide Deposits, H. Ohmoto and B.J. Skinner, eds., Econ. Geol. Monogr. 5, pp. 184–197, 1983.

14 D.C. Rhodes, R.A. Lutz, E.C. Revelas and R.M. Cerrato, Growth rates of bivalves at deep-sea hydrothermal vents along the Galapagos Rift, Science 214, 911–912, 1981.

15 K.K. Turekian and J.K. Cochran, Growth rates of a vesicomyid clam from the Galapagos spreading center, Science 214, 909–911, 1981.

16 K.K. Turekian, J.K. Cochran and J.T. Bennett, Growth rate of a vesicomyid clam from the 21°N East Pacific Rise hydrothermal area, Nature 303, 55–56, 1983.

17 S. Krishnaswami and K.K. Turekian, ^{238}U, ^{226}Ra and ^{210}Pb in some vent waters from the Galapagos Spreading Center, Geophys. Res. Lett. 9, 827–830, 1982.

18 W.R. Normark, J.L. Morton, R.A. Koski, D.A. Clague and J.R. Delaney, Active hydrothermal vents and sulfide deposits on the southern Juan de Fuca Ridge, Geology 11, 158–163, 1983.

19 J.R. Delaney, H.P. Johnson and J.L. Karsten, The Juan de Fuca Ridge hot spot—propagating rift system: new tectonic, geochemical, and magnetic data, J. Geophys. Res. 86, 11747–11750, 1981.

20 H.P. Johnson, J.L. Karsten, J.R. Delaney, E.E. Davis, R.G. Currie and R.L. Chase, A detailed study of the Cobb Offset of the Juan de Fuca Ridge: Evolution of a propagating rift, J. Geophys. Res. 88, 2297–2315, 1983.

21 M.K. Tivey and J.R. Delaney, Sulfide deposits from the Endeavour Segment of the Juan de Fuca Ridge, Mar. Min., in press.
22 M.K. Tivey and J.R. Delaney, Growth of large sulfide structures on the Endeavour segment of the Juan de Fuca Ridge, submitted to Earth Planet. Sci. Lett., 1985.
23 W.S. Broecker, The application of natural radon to problems in ocean circulation, in: Symposium of Diffusion in Ocean and Fresh Water, T. Ichiye, ed., pp. 116–145, Lamont-Doherty Geological Observatory, Palisades, N.Y., 1965.
24 G. Kipphut, An investigation of sedimentary processes in lakes, Ph.D. Thesis, Columbia University, New York, N.Y., 1978.
25 M. Tatsumoto and D.M. Unruh, KREEP basalt age: Grain by grain U-Th-Pb systematics study of quartz monzonite clast 15405, 88, Proc. 7th Lunar Sci. Conf., pp. 2107–2129, 1976.
26 S. Newman, R.C. Finkel and J.D. Macdougall, ^{230}Th-^{238}U disequilibrium systematics in oceanic tholeiites from 21°N on the East Pacific Rise, Earth Planet. Sci. Lett. 65, 17–33, 1983.
27 R.M. Haymon and M. Kastner, Hot spring deposits on the East Pacific Rise at 21°N: preliminary description of mineralogy and genesis, Earth Planet. Sci. Lett. 53, 363–381, 1981.
28 M.M. Styrt, A.J. Brackmann, H.D. Holland, B.C. Clark, V. Pisutha-Armond, C.S. Eldridge and H. Ohmoto, The mineralogy and the isotopic composition of sulfur in hydrothermal sulfide/sulfate deposits on the East Pacific Rise, 21°N latitude, Earth Planet. Sci. Lett. 53, 382–390, 1981.
29 E. Oudin, Hydrothermal sulfide deposits of the East Pacific Rise (21°N), I. Descriptive mineralogy, Mar. Min. 4, 39–72, 1983.
30 R.H. Haymon, The growth history of black smoker chimneys, Nature 301, 695–698, 1983.
31 P.H. Vidal and N. Clauer, Pb and Sr isotopic systematics of some basalts and sulfides from the East Pacific Rise at 21°N (Project RITA), Earth Planet. Sci. Lett. 55, 237–246, 1981.
32 J. Dymond, R. Cobler, L. Gordon, P. Biscaye and C. Mathieu, ^{226}Ra and ^{222}Rn contents of Galapagos Rift hydrothermal waters—the importance of low-temperature interactions with crustal rocks, Earth Planet. Sci. Lett. 64, 417–429, 1983.
33 K. Kim and R.C. Finkel, Radioactivities on 21°N hydrothermal system, EOS, Trans. Am. Geophys. Union 61, 995, 1980.
34 D. Kadko and J.E. Lupton, Radon-222 and temperature measurements on the Endeavour Ridge, EOS, Trans. Am. Geophys. Union 65, 974, 1984.
35 S.T. Church and M. Tatsumoto, Lead isotope relations in oceanic ridge basalts from the Juan de Fuca, Gorda area, N.E. Pacific Ocean, Contrib. Mineral. Petrol. 53, 253–279, 1975.
36 C.J. Allègre and M. Condominis, Basalt genesis and mantle structure studied through Th-isotopic geochemistry, Nature 299, 21–24, 1982.
37 D. Elvers, K. Potter, D. Scidel and J. Morley, I.D.O.E. Survey or Seamap, N.O.S. seamap profiles plates BGM-1-71. NOAA Environmental Data Service, Washington, D.C.